Chemical Physics Letters 561–562 (2013) 52–56

Contents lists available at SciVerse ScienceDirect

Chemical Physics Letters

journal homepage: www.elsevier.com/locate/cplett

Energy transfer and phosphorescence-quenching dynamics in a phosphorescent host–guest system

Chih-Wei Chang [a,*], Rei-Yun Lee [b], Eric Wei-Guang Diau [b,*]

[a] Department of Chemistry, National Changhua University of Education, Changhua 50058, Taiwan
[b] Department of Applied Chemistry and Institute of Molecular Science, National Chiao Tung University, Hsinchu 30010, Taiwan

ARTICLE INFO

Article history:
Received 18 August 2012
In final form 20 January 2013
Available online 6 February 2013

ABSTRACT

We investigated the energy transfer dynamics in a phosphorescent host–guest system. Two spirobifluorene derivatives, [2,7-bis(2,2-diphenylvinyl)-9,9′-spirobifluorene] (DPVSBF) and [2,7-bis(1,2,2-triphenylvinyl)-9,9′-spirobifluorene] (TPVSBF), were doped with the red phosphor complex [Os(bpftz)$_2$(PPh$_2$Me)$_2$] (Os-R). The two hosts exhibit similar host-to-guest energy transfer efficiencies; however, the backward energy transfer from the Os-R complex to TPVSBF is slower than that from Os-R to DPVSBF. Quantum chemical calculations suggest that the backward energy transfer dynamics are related to the host's triplet-state energy level. The greater energy of the TPVSBF triplet state compared to that of DPVSBF plays a crucial role in its ability to confine triplet excitons in Os-R.

1. Introduction

After the first report of an organic electroluminescent diode in 1987 [1], much effort has been devoted to developing organic light-emitting diodes (OLED) [2]. The OLED has applications in flat panel displays, and is promising as the next-generation solid-state lighting device [3,4]. The external quantum efficiency (η_{ext}) of the OLED is determined by its internal quantum yield (η_{int}) and the light out-coupling efficiency (η_{ph}) [5]:

$$\eta_{ext} = \eta_{int}\eta_{ph} = \gamma\eta_{ex}\phi_p\eta_{ph} \quad (1)$$

The internal quantum yield comprises the electron–hole charge-balance factor (γ), the fraction of total excitons that produce radiation (η_{ex}), and the intrinsic radiative quantum efficiency of the emitter (φ_p). The theoretical value of the light out-coupling efficiency for an OLED with a glass substrate is approximately 20% [2]. Only singlet excitons can be used to generate photons in a fluorescent emitter. The formation of singlet and triplet excitons by random exciton formation occurs in a ratio of 1:3; thus, a fluorescence emitter can provide a maximum η_{ex} ratio of 0.25. In a phosphorescent emitter, photons can be generated from either singlet or triplet excitons, and this capacity increases the theoretical η_{ex} ratio to 1; a phosphorescent OLED with nearly 100% internal quantum yield has been reported [6]. The prevailing strategy for fabricating OLEDs is to dope an electron transfer layer (host) with phosphors (guests) [6–9]. This approach significantly improves OLED efficiency because it effectively suppresses aggregation quenching and triplet–triplet annihilation of the phosphorescence emitter [10]. In this Letter, we doped two novel blue-light-emitting host materials: [2,7-bis(2,2-diphenylvinyl)-9,9′- spirobifluorene] (DPVSBF) and [2,7-bis(1,2,2-triphenylvinyl)-9,9′-spirobifluorene] (TPVSBF) [11,12] with the red phosphor [Os(bpftz)$_2$(PPh$_2$Me)$_2$] (Os-R) (Scheme 1) [13]. The structures of DPVSBF and TPVSBF resemble that of the well-known blue-light-emitting material, 4,4′-bis(2,2′-diphenylvinyl)-1,1′-biphenyl. In DPVSBF, bis(2,2′-diphenylvinyl) moieties are connected at the 2 and 7 positions of 9,9′-spirobifluorene, whereas in TPVSBF, these positions are substituted with bis(1,2,2-triphenylvinyl). The presence of a rigid spirobifluorene moiety significantly increases the glass transition temperature and extends the operational lifetimes of the devices [11,12].

Various energy transfer processes are involved in transporting excitons in a host–guest system [14]. It is essential for designers to understand energy transfer dynamics to prevent unwanted energy loss in OLED devices, and to control the color quality of white-light OLEDs [15]. Energy transfer dynamics in OLED devices can be measured using time-resolved electroluminescence (EL) or time-resolved photoluminescence (PL) systems. For time-resolved EL measurements, singlet and triplet excitons are generated simultaneously, and interpretation of the observed dynamics is complex. In this Letter, we adopted a time-resolved PL system, which enabled selectively exciting singlet-state exitons in the host and probing the subsequent energy transfer dynamics in the host–guest system. Our results suggest that the host's triplet-state energy is important for controlling the backward energy transfer processes, and has a close relationship with the phosphor emission efficiency in the OLED.

* Corresponding authors.
E-mail addresses: cwchang@cc.ncue.edu.tw (C.-W. Chang), diau@mail.nctu.edu.tw (E.W-G. Diau).

0009-2614/$ - see front matter © 2013 Elsevier B.V. All rights reserved.
http://dx.doi.org/10.1016/j.cplett.2013.01.038

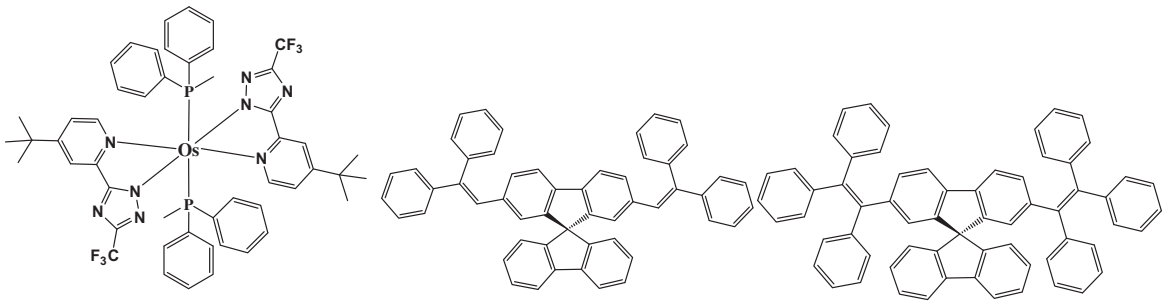

Scheme 1.

2. Experimental

2.1. Steady-state spectrometry and thin-film sample preparation

Absorption spectra were acquired using a Cary 50 UV–Vis spectrophotometer. Emission spectra were obtained using a Hitachi F4500 spectrophotometer. The synthesis and identification of Os-R, DPVSBF, and TPVSBF were performed as previously reported [11–13]. The spectra of samples in solution were measured directly in standard 1 cm cuvettes. Thin-film samples were placed on a designated solid-state sample holder. Vacuum deposited films ($<5 \times 10^{-6}$ Torr) were prepared on quartz glass substrates using an Auto168 vacuum evaporator (Junsun Tech co., LTD). The deposition rates and film thickness were controlled to 1 Å/s and 30 nm, respectively. Poly(methyl methacrylate) (PMMA) film samples were prepared by mixing PMMA in chloroform with 2% Os-R, and then spin-coating onto quartz glass.

2.2. Picosecond time-resolved spectroscopy

Picosecond time-resolved spectra were obtained using a time-correlated single-photon counting (TCSPC) system (Fluotime 200, PicoQuant). The excitation wavelength was fixed at 375 nm for all experiments. For DPVSBF and TPVSBF film decays, the excitation source was a vertical polarized picosecond pulsed-diode laser (LDH-375, PicoQuant, FWHM approximately 70 ps, repetition rate = 40 MHz, photon density = 3.8×10^{10} photons/cm^2 per pulse) controlled by a picosecond pulsed laser driver (PDL800-D, PicoQuant). For the phosphorescence decays of DPVSBF + Os-R and TPVSBF + Os-R films, the excitation source was a frequency-doubled femtosecond mode-locked Ti:Sapphire laser (Coherent, Mira 900D). The repetition rates of the femtosecond laser were reduced to 0.5 MHz by a pulse picker (Coherent, Model 9200) to avoid multiple excitations. The excitation power for the frequency-doubled Ti:sapphire laser was attenuated to minimize sample degradation (photon density = 3×10^{12} photons/cm^2 per pulse). Thin-film samples were placed on a custom-designed solid-state sample holder, and the incident light angle was set to 45°. A lens focused the excitation beam, whereas a second lens, set at a right angle, collected the fluorescence emission from the sample. An iris attenuated the detected signal intensity to ensure that the counting rate was less than 1/100 of the laser repetition rate. The polarization of the detected fluorescence relative to the excitation laser pulse was set at the magic angle, 54.7°, using a polarizer. A double monochromator was used to compensate for the signal's group velocity dispersion, and select the detection wavelength. A multichannel-plate photomultiplier was connected to a computer through a TCSPC-module card (SPC-630, Becker and Hickl) for data acquisition.

2.3. Computational method

The ground-state structures of DPVSBF and TPVSBF were optimized using G03 software [16] at the B3LYP/6-31G(d) level of theory. The vertical excitation energies of the optimized structures were calculated using the time-dependent density function theory (TDDFT) method at the same level.

3. Results and discussion

3.1. Steady state absorption and emission spectra

Figure 1a shows the steady-state spectra for DPVSBF. The absorption and emission bands in the CH_2Cl_2 solution are centered on 375 and 450 nm, respectively. The DPVSBF film absorption spectrum is red-shifted to 383 nm, and the corresponding emission is red-shifted to 460 nm. The bathochromic shift seen in the spec-

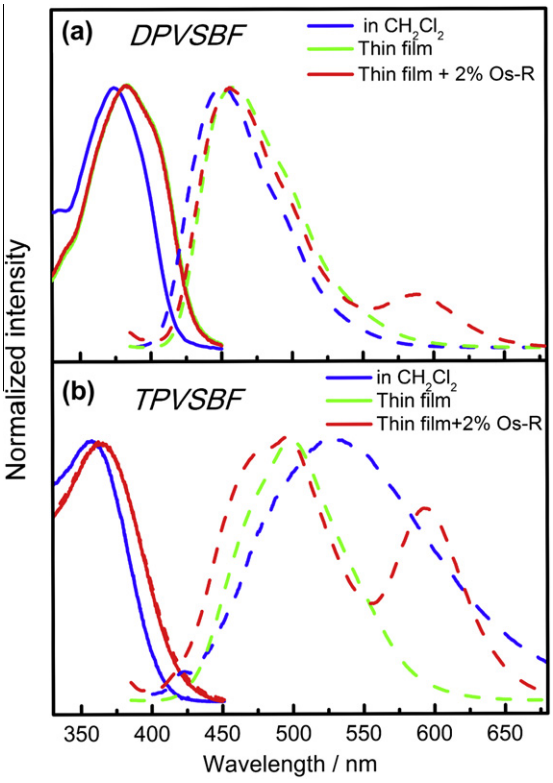

Figure 1. The normalized steady state spectra of (a) DPVSBF and (b) TPVSBF. The excitation wavelength for the emission spectra was fixed at 375 nm for all samples. The inset shows raw data for the emission spectra.

tra is a result of matrix effects in the solid film. Figure 1b shows absorption and emission spectra for TPVSBF. In CH_2Cl_2, the absorption and emission bands are centered on 358 and 530 nm, respectively. The Stokes shift of TPVSBF in CH_2Cl_2 is significantly greater than that of DPVSBF, suggesting that TPVSBF has a greater structural difference between the excited and ground states than DPVSBF has. The TPVSBF solid film absorption is also red-shifted to 364 nm because of matrix effects. However, the Stokes shift for the TPVSBF solid film is significantly smaller than that seen in solution; hence, the TPVSBF emission is contrariwise blue-shifted to approximately 500 nm. We attributed the observed decrease in Stokes shift for the solid film to the restriction of large amplitude motions in the solid state. In the 2% Os-R doped film, the host fluorescence is diminished (Fig. S1) because of energy transfer from the host to Os-R. The small emission band at approximately 590 nm arises from emission by Os-R (Figure 1). To evaluate direct emission by the host, we measured the emission of the 2% Os-R doped PMMA film (Fig. S1). The Os-R emission was significantly enhanced in host–guest films, indicative of excitation energy transfer from the host to Os-R.

The fluorescence (or phosphorescence) quantum yield (Φ_F) can be calculated using the following equation:

$$\Phi_F \propto \frac{\int_0^\infty I_F(\lambda_E, \lambda_F)d\lambda}{I_0(\lambda_E) \times [1 - 10^{-A(\lambda_E)}]} \quad (2)$$

The $\int_0^\infty I_F(\lambda_E, \lambda_F)d\lambda$ term represents the integral of the fluorescence spectrum obtained by excitation at λ_E. For the 2% Os-R doped films, we deconvoluted the signals originating from the host and Os-R by lognormal fitting (Figs. S2 and S3), and thus, calculated their integrals separately. The $I_0(\lambda_E)$ term represents the intensity of excitation light, and should be constant for all samples. $A(\lambda_E)$ is the absorbance of the sample at excitation wavelength λ_E. Based on Eq. (2), the fluorescence quantum-yield ratio between any two films is given by

$$\frac{\Phi_{film1}}{\Phi_{film2}} = \frac{\int_0^\infty I_{film1}(\lambda_E, \lambda_F)d\lambda}{\int_0^\infty I_{film2}(\lambda_E, \lambda_F)d\lambda} \times \frac{[1 - 10^{-A(\lambda_E)_{film2}}]}{[1 - 10^{-A(\lambda_E)_{film1}}]} \quad (3)$$

The results are summarized in Table 1. To address the issue of energy transfer dynamics in these films, we measured a series of time-resolved fluorescence transients, and these results are discussed in the following section.

3.2. Forward energy transfer dynamics in DPVSBF and TPVSBF host–guest systems

Figure 2 shows time-resolved fluorescence transients for DPVSBF and TPVSBF films, and for the corresponding Os-R doped films. The transients are fitted with a bi-exponential decay function, and the fitting parameters are tabulated in Table 1. To compare the fluorescence decays between films, the average fluorescence lifetime is calculated by

$$\tau_{average} = \frac{\sum_{i=1}^{2} Amp_i \times \tau_i}{\sum_{i=1}^{2} Amp_i} \quad (4)$$

where Amp_i and τ_i represent the amplitude and the lifetime of each component, respectively. In the host film, the reciprocal of the aver-

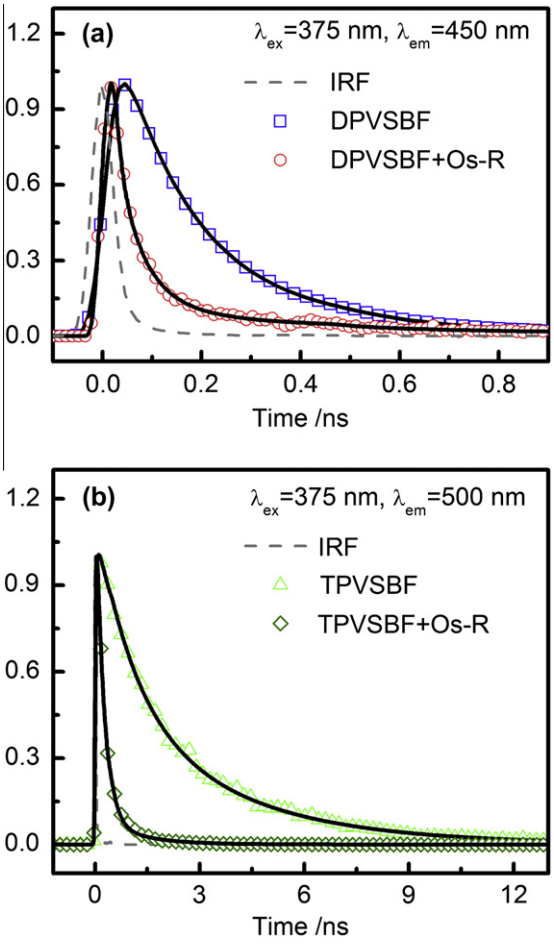

Figure 2. The picosecond time-resolved fluorescence transients of (a) DPVSBF and (b) TPVSBF film excited at 375 nm. The grey dashed line indicates the instrument response function. In both cases, the fluorescence decay rate is significantly increased in the 2% Os-R doped films, resulting in severe fluorescence quenching in these films.

Table 1
Steady state fluorescence intensity and parameters for time-resolved fluorescence decays of DPVSBF, TPVSBF and the corresponding Os-R doped films.

	DPVSBF	DPVSBF + 2% Os-R	TPVSBF	TPVSBF + 2% Os-R
Absorbance (375 nm)	0.203	0.170	0.142	0.140
$\int_0^\infty I^{host}(\lambda_F)d\lambda_F$	128 000	13 700	433 000	54 000
$\int_0^\infty I^{Os\text{-}R}(\lambda_p)d\lambda_p$	N.A.	3100	N.A.	26 700
τ_1 (%)	0.15 ns (87%)	0.025 ns (97%)	1.05 ns (53%)	0.26 ns (96%)
τ_2 (%)	0.46 ns (13%)	0.3 ns (3%)	3.45 ns (47%)	1.7 ns (4%)
[a] $\tau_{avg.}$	0.19 ns	0.033 ns	2.18 ns	0.32 ns
[b] k_{ET}/s^{-1}	2.50×10^{10}		2.67×10^{9}	
[c] $\Phi_F^{host+Os\text{-}R}/\Phi_F^{host}$	0.124		0.127	
[c] $\Phi^{DPVSBF}/\Phi^{TPVSBF}$	0.22			
$E_{host \to Os\text{-}R}/I_0(\lambda_E)$	0.284		0.239	

[a] The value is calculated based on Eq. (4).
[b] The value is calculated based on Eq. (7).
[c] The value is obtained from Eq. (3).

age fluorescence lifetime is the sum of the radiative (k_r) and non-radiative (k_{nr}) rate coefficients:

$$\frac{1}{\tau_{avg}^{host}} = k_r + k_{nr} \quad (5)$$

In the Os-R doped film, the average fluorescence lifetime decreases substantially because of the contribution of energy transfer from the host to Os-R. Thus, the average fluorescence lifetime for Os-R films is given by

$$\frac{1}{\tau_{avg}^{host+Os-R}} = k_r + k_{nr} + k_{ET} \quad (6)$$

where k_{ET} is the energy transfer rate from the host to Os-R. Eqs. (5) and (6) provide

$$k_{ET} = \frac{1}{\tau_{avg}^{host+Os-R}} - \frac{1}{\tau_{avg}^{host}} \quad (7)$$

As shown in Table 1, the DPVSBF to Os-R k_{ET} value is $2.50 \times 10^{10}\ s^{-1}$, and k_{ET} for the TPVSBF to Os-R transition is $2.67 \times 10^{9}\ s^{-1}$. The $k_{ET}^{DPVSBF \to Os\text{-}R}$: $k_{ET}^{TPVSBF \to Os\text{-}R}$ ratio is 9.36.

In our system, the host-to-guest energy transfer occurs between the singlet excited-state of the DPVSBF or TPVSBF host, and the singlet excited-state of Os-R. In this singlet–singlet energy transfer process, energy can transfer through either dipole–dipole interactions (Förster mechanism) or by orbital overlap (Dexter mechanism) interactions [17]. The long-range Förster mechanism is generally dominant for singlet–singlet energy transfer processes [18]. From the steady-state absorption and emission spectra, the $\frac{k_{ET}^{DPVSBF \to Os\text{-}R}}{k_{ET}^{TPVSBF \to Os\text{-}R}}$ ratio of the energy transfer rate, estimated based on Förster energy transfer theory, is 9.94 (see supporting information for the derivation). The result is in agreement with the value obtained from the lifetime measurement of 9.36. Although we cannot form a definite conclusion for the energy transfer mechanism based on this result, our findings suggest that the Förster dipole–dipole energy transfer mechanism plays a major role in the host-to-guest energy transfer process. Additionally, we found no evidence that the Dexter mechanism is important for the system under study.

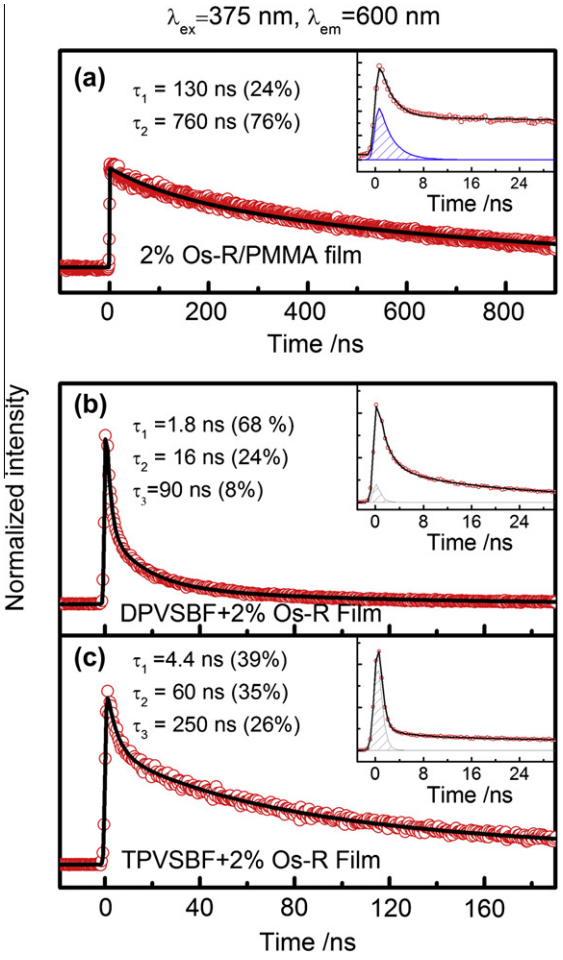

Figure 3. The time-resolved phosphorescence transients of Os-R doped with (a) PMMA (b) DPVSBF (c) TPVSBF at an excitation wavelength of 375 nm and emission wavelength of 600 nm for all samples. The inset shows raw data for the transients. The interferences from PMMA and host fluorescence are represented by the blue and grey curves, respectively.

3.3. Backward energy transfer dynamics in DPVSBF and TPVSBF host–guest systems

In our two host–guest films, the phosphorescence integral, $\int_0^\infty I^{Os\text{-}R}(\lambda_p)d\lambda_p$, of the Os-R doped TPVSBF film is 8.6 times greater than than that of the Os-R doped DPVSBF film (Fig. S1 and Table 1). In a phosphorescent host–guest system, the phosphorescence intensity of the guest, which in this Letter is Os-R, is determined by two factors: energy transfer from the host, and the phosphorescence quantum yield of the guest. The energy transferred from the host to the guest is estimated using the following equation:

$$E_{host->Os\text{-}R} = I_0(\lambda_E)(1 - 10^{-A(\lambda_E)}) \times \left(1 - \frac{\Phi_{host+Os\text{-}R}}{\Phi_{host}}\right) \quad (8)$$

The results shown in Table 1 suggest that DPVSBF and TPVSBF have similar energy transfer efficiencies. Therefore, the difference in Os-R emission intensity between these films must arise from differences in the phosphorescence quantum yields. To investigate this, we measured the phosphorescence decays of pure Os-R and the two Os-R doped hosts. To avoid phosphorescence quenching caused by intermolecular aggregation, we added 2% Os-R to PMMA and spin-coated the mixture onto quartz glass. Figure 3 shows Os-R phosphorescence decays probed at 600 nm. In the PMMA film (Figure 3a), the initial fast component (blue curve, inset) closely resembles the decay of pure PMMA film (Fig. S5), and thus, we ascribed this decay spectrum to the PMMA emission (Fig. S5). In the 2% Os-R doped DPVSBF and TPVSBF films (Figure 3b and c), the initial fast component (grey curve, inset) is similar to the fluorescence decay spectrum of the host measured at a shorter wavelength (Fig. S5); therefore, we attributed this component to residual fluorescence of the host. For clarity, Figure 3 only shows transient signals after removal of these interferences. The multi-exponential fitting parameters of these transients are summarized in Table 2. The results indicate that the presence of a host complex will substantially quench the Os-R phosphorescence. Similar phosphorescence-quenching dynamics were reported for Ir-complex emitters doped in polymer host materials [19–21]. Previous literature reports suggest that phosphorescence quenching arises from backward guest-to-host energy transfer, and the degree of phosphorescence quenching is closely related to the triplet-state energy of the polymer matrix [19–21]. To test the validity of this model, the triplet-state energies of DPVSBF and TPVSBF were estimated using quantum chemical calculation methods. We optimized the DPVSBF and TPVSBF structures at the B3LYP/6-31g* level of theory, and calculated the vertical excitation energy using TDDFT method at the same level. The results are summarized in Table S1. The DPVSBF and TPVSBF absorption bands, 3.31 and 3.47 eV, respectively, were used to check the validity of our calculation. Although the quantum chemical calculation systemically underestimated the excitation energy by approximately 0.28 eV, the absorption

Table 2
Fitting parameters for the time-resolved phosphorescence transients of Os-R doped in PMMA, DPVSBF and TPVSBF films.

	PMMA	DPVSBF + 2% Os-R	TPVSBF + 2% Os-R
τ_1 (%)	130 ns (24)	1.8 ns (68)	4.4 ns (39)
τ_2 (%)	760 ns (76)	16 ns (24)	60 ns (35)
τ_3 (%)		90 ns (8)	250 ns (26)
$\tau_{avg.}$	609 ns	12.3 ns	88 ns
[a] $k_{BET}^{Os-R\rightarrow host}/s^{-1}$		7.97×10^7	9.7×10^6

$\left(\frac{1}{\tau_{avg}^{host+2\%Os\text{-}R}} = k_r^{Os\text{-}R} + k_{nr}^{Os\text{-}R} + k_{BET}^{Os\text{-}R\rightarrow host}, \frac{1}{\tau_{avg}^{Os\text{-}R}} = k_r^{Os\text{-}R} + k_{nr}^{Os\text{-}R}\right)$.

[a] $k_{BET}^{Os\text{-}R\rightarrow host}$ is equal to $\frac{1}{\tau_{avg}^{host+2\%Os\text{-}R}} - \frac{1}{\tau_{avg}^{Os\text{-}R*}}$.

energy's qualitative trend is in good agreement with our experimental values. The $S_0 \rightarrow T_1$ excitation energy is predicted to be 2.08 eV for DPVSBF and 2.30 eV for TPVSBF (Table S1). The backward energy transfer rates from Os-R to DPVSBF and from Os-R to TPVSBF are estimated as 7.97×10^7 and 9.70×10^6 s^{-1}, respectively. This result suggests that the greater triplet-state energy of TPVSBFs is crucial for confining the triplet exciton on Os-R, and results in increased Os-R emission intensity and slower backward energy transfer rates in 2% Os-R doped TPVSBF films.

4. Conclusion

We reported the complete characterization of forward and backward energy transfer dynamics in an OLED host–guest system. Time-resolved PL spectroscopy enabled estimation of the energy transfer rate from DPVSBF to Os-R as 2.5×10^{10} s^{-1} and from TPVSBF to Os-R as 2.67×10^9 s^{-1}. The measured energy-transfer rate ratio is in agreement with the value predicted by the Förster energy transfer model. Although the observed host-to-guest energy transfer efficiencies of these two films are similar, the phosphorescence intensity of the Os-R doped TPVSBF film is 8.6 times higher than that of the Os-R doped DPVSBF film because of the significantly lower backward energy transfer rates seen for the Os-R to TPVSBF energy transfer. Our quantum chemical calculation results suggest that a backward energy transfer from Os-R to TPVSBF is slowed because of the greater triplet-state energy of TPVSBF. Our study found that the energy of the low-lying triplet state of the host is an important factor in the phosphorescence-quenching dynamics of Os-based phosphorescent emitters. This finding is consistent with previous reports, in which the phosphorescence-quenching dynamics of Ir-based complexes were found to be closely related to the triplet-state energy of the host [19–21]. Our study revealed that backward guest-to-host energy transfer is a general phosphorescence-quenching mechanism in host–guest OLED systems, and this should be considered when designing host materials for OLEDs.

Acknowledgments

C.-W. Chang thanks the National Science Council of Taiwan for financial support under project contracts: 100-2113-M-018-005-MY2. Eric W.G. Diau would like to thank the National Science Council of Taiwan and the Ministry of Education of Taiwan who provided support for this project under the ATU program.

Appendix A. Supplementary data

Supplementary data associated with this article can be found, in the online version, at http://dx.doi.org/10.1016/j.cplett.2013.01.038.

References

[1] C.W. Tang, S.A. VanSlyke, Appl. Phys. Lett. 51 (1987) 913.
[2] L.X. Xiao, Z.J. Chen, B. Qu, J.X. Luo, S. Kong, Q.H. Gong, J.J. Kido, Adv. Mater. 23 (2011) 926.
[3] S. Tasch et al., Appl. Phys. Lett. 71 (1997) 2883.
[4] T. Fuhrmann, J. Salbeck, MRS Bull. 38 (2003) 354.
[5] C. Adachi, M.A. Baldo, M.E. Thompson, S.R. Forrest, J. Appl. Phys. 90 (2001) 5048.
[6] M.A. Blado, D.F. O'Brien, Y. You, A. Shoustikov, S. Sibley, M.E. Thompson, S.R. Forrest, Nature 395 (1998) 151.
[7] C.W. Tang, S.A. VanSlyke, C.H. Chen, J. Appl. Phys. 65 (1989) 3610.
[8] M.A. Baldo, S. Lamansky, P.E. Burrows, M.E. Thompson, S.R. Forrest, Appl. Phys. Lett. 75 (1999) 4.
[9] C. Adachi, M.A. Baldo, S.R. Forrest, S. Lamansky, M.E. Thompson, Appl. Phys. Lett. 78 (2001) 1622.
[10] M.A. Baldo, C. Adachi, S.R. Forrest, Phys. Rev. B 62 (2000) 10967.
[11] F.-I. Wu, C.-F. Shu, T.-T. Wang, E.W.-G. Diau, C.-H. Chien, C.-H. Chuen, Y.-T. Tao, Synth. Met. 151 (2005) 285.
[12] C.H. Chuen, Y.T. Tao, F.I. Wu, C.F. Shu, Appl. Phys. Lett. 85 (2004) 4609.
[13] P.-I. Shih, C.-F. Shu, Y.-L. Tung, Y. Chi, Appl. Phys. Lett. 88 (2006) 251110.
[14] M.A. Baldo, D.F. O'brien, Phys. Rev. B 60 (1999) 14422.
[15] C. Weichsel, S. Reineke, M. Furno, B. Lüssem, K. Leo, J. Appl. Phys. 111 (2012) 033102.
[16] M.J. Frisch, G.W. Trucks, H.B. Schlegel, G.E. Scuseria, M.A. Robb, J.R. Cheeseman, J. Montgomery, J.A.T. Vreven, K.N. Kudin, J.C. Burant, J.M. Millam, S.S. Iyengar, J. Tomasi, V. Barone, B. Mennucci, M. Cossi, G. Scalmani, N. Rega, G.A. Petersson, H. Nakatsuji, M. Hada, M. Ehara, K. Toyota, R. Fukuda, J. Hasegawa, M. Ishida, T. Nakajima, Y. Honda, O. Kitao, H. Nakai, M. Klene, X. Li, J.E. Knox, H.P. Hratchian, J.B. Cross, V. Bakken, C. Adamo, J. Jaramillo, R. Gomperts, R.E. Stratmann, O. Yazyev, A.J. Austin, R. Cammi, C. Pomelli, J.W. Ochterski, P.Y. Ayala, K. Morokuma, G.A. Voth, P. Salvador, J.J. Dannenberg, V.G. Zakrzewski, S. Dapprich, A.D. Daniels, M.C. Strain, O. Farkas, D.K. Malick, A.D. Rabuck, K. Raghavachari, J.B. Foresman, J.V. Ortiz, Q. Cui, A.G. Baboul, S. Clifford, J. Cioslowski, B.B. Stefanov, G. Liu, A. Liashenko, P. Piskorz, I. Komaromi, R.L. Martin, D.J. Fox, T. Keith, M.A. Al-Laham, C.Y. Peng, A. Nanayakkara, M. Challacombe, P.M.W. Gill, B. Jhonson, W. Chen, M.W. Wong, C. Gonzalez, J.A. Pople, Gaussian, Inc., Wallingford CT, 2004.
[17] B. Valeur, Molecular Fluorescence, Wiley-VCH, New York, 2002.
[18] D.F. O'brien, M.A. Baldo, M.E. Thompson, S.R. Forrest, Appl. Phys. Lett. 74 (1999) 442.
[19] F.-C. Chen, G. He, Y. Yang, Appl. Phys. Lett. 82 (2003) 1006.
[20] M. Sudhakar, P.I. Djurovich, T.E. Hogen-Esch, M.E. Thompson, J. Am. Chem. Soc. 125 (2003) 7796.
[21] J. An et al., J. Photochem. Photobiol. A 200 (2008) 371.